CHEMISTRY
A EUROPEAN JOURNAL

FULL PAPER

DOI: 10.1002/chem.201303115

# Synthesis and Bonding in Carbene Complexes of an Unsymmetrical Dilithio Methandiide: A Combined Experimental and Theoretical Study

Viktoria H. Gessner,*[a] Florian Meier,[b] Diana Uhrich,[a] and Martin Kaupp*[b]

**Abstract:** Herein, we report the preparation of a new unsymmetrical, bis-(thiophosphinoyl)-substituted dilithio methandiide and its application for the synthesis of zirconium- and palladium-carbene complexes. These complexes were found to exhibit remarkably shielded $^{13}C$ NMR shifts, which are much more highfield-shifted than those of "normal" carbene complexes. DFT calculations were performed to determine the origin of these observations and to distinguish the electronic structure of these and related carbene complexes compared with the classical Fischer and Schrock-type complexes. Various methods show that these systems are best described as highly polarized Schrock-type complexes, in which the metal–carbon bond possesses more electrostatic contributions than in the prototype Schrock systems, or even as "masked" methandiides. As such, geminal dianions represent a kind of "extreme" Schrock-type ligands favoring the ionic resonance structure $M^+-CR_2^-$ as often used in textbooks to explain the nucleophilic nature of Schrock complexes.

**Keywords:** carbenes · density functional calculations · dianions · lithium · transition metals

## Introduction

Transition-metal carbene complexes have experienced huge interest over the past decades due to their many applications in both stoichiometric and catalytic organic transformations. It is well-known that the nature and reactivity of the carbene complexes greatly depends on the electronic properties of the substituents bound to the carbine-carbon atom. Those with hydrogen- or alkyl/aryl substituents are usually classified as Schrock carbenes (alkylidenes), whereas those containing electronegative heteroatom substituents, such as O, N, or S, are designated as Fischer carbenes.[1] In recent years, bis(phosphonium)-stabilized methandiides have received increasing interest as precursors for new carbene complexes.[2] These complexes were reported to exhibit unique electronic properties differing from the generally known Fischer-type carbene and the Schrock-type alkylidene complexes.[3] So far, this research has mainly focused on the oxidized versions of the commercially available bis-(diphenylphosphino)methane (DPPM) ligand. The groups of Cavell and Liddle studied the coordination chemistry of the bis(iminophosphorane) derivative in depth, whereas Le Floch, Mézailles, and co-workers focused on the thiophosphinoyl congeners. Hence, a huge variety of different transition-metal carbene complexes (incorporating early (e.g., Ti, Zr, Hf) and late transition-metals (e.g., Pd, Pt)) that also complex with lanthanides and actinides, have been prepared.[4] These complexes revealed interesting, partly different reactivities depending on the ligand and the metal center. As such, metallo-Wittig-like reactivity was observed in reactions of zirconium and scandium complexes with carbonyl compounds,[5] whereas C–H bond activation was observed with an yttrium complex.[6]

Although quite a number of carbene complexes derived from dilithio methandiides has been synthesized over the past years, the bonding situation is still under debate. Only recently, Mindiola and Scott highlighted the differences of theses carbene complexes compared with the typical Fischer and Schrock complexes.[3] Formally, the bonding situation in these complexes can be described by a four-electron donation from the ligand to the metal, leaving a negatively charged carbon atom bound to electron-withdrawing substituents (Figure 1).[2] Although these carbenes were often reported to possess Schrock/alkylidene-like reactivity, no comparative study of the electronic structure has been undertaken to rank these complexes within the Fischer and Schrock classification Scheme.[4k] Thus the question arises, whether carbene complexes derived from dilithio methandiides indeed display a new class of carbene complexes as depicted in Figure 1; or, do they simply offer a new route to Schrock alkylidenes, which also allows for the syntheses of complexes with late transition-metals in low oxidation states.

It should be noted that also the terms Fischer- and Schrock-type complexes have been used differently in litera-

[a] Dr. V. H. Gessner, D. Uhrich
Institut für Anorganische Chemie
Julius-Maximilians-Universität Würzburg
Am Hubland, 97074 Würzburg (Germany)
E-mail: vgessner@uni-wuerzburg.de

[b] F. Meier, Prof. Dr. M. Kaupp
Technische Universität Berlin, Institut für Chemie
Sekr. C7, Strasse des 17. Juni 135
10623 Berlin (Germany)
E-mail: martin.kaupp@tu-berlin.de

Supporting information for this article is available on the WWW under http://dx.doi.org/10.1002/chem.201303115.

  

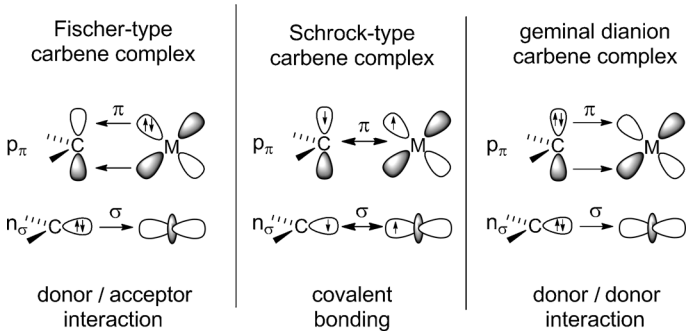


Figure 1. Representation of the dominant orbital interactions in a) Fischer-type carbenes, b) Schrock-type alkylidenes, and c) complexes based on methandiides.

ture. This originates from the fact that classifications according to textbook descriptions (Fischer-type: π-donor substituents, metals in low oxidation states, electrophilic character) are often ambiguous and the transitions are smooth. As such, complexes have been reported featuring a metal center in low oxidation state (Fischer-type), but with nucleophilic character and thus Schrock-type reactivity. Alternatively, both types of complexes were distinguished by the bonding situation. Thus, Fischer-carbenes were described to be formed by donor–acceptor interactions of singlet fragments, whereas Schrock-alkylidenes bind covalently as triplet species.[7] Additionally, distinction solely by means of the oxidation state of the metal or the type of substituents at the carbene carbon atom are made. Because of the focus of this paper on the influence of the methandiide ligand systems on the bonding situation, we decided to use the terms Schrock and Fischer complexes depending on the α-substituents.

In this publication, we describe the synthesis of an unsymmetrical dilithio methandiide and its application as a ligand in transition-metal carbene complexes. We have chosen zirconium as the early- and palladium as the late-metal center to compare their influence on the bonding situation. In the course of these studies, we observed remarkably shielded $^{13}C$ NMR shifts, which prompted us to perform detailed computational studies to understand these observations and especially to distinguish the bonding situation in these systems from known Fischer and Schrock complexes. To gain insight into the electronic structure, electron localization function (ELF), atoms in molecules (AIM) and natural bond orbital (NBO) analyses have been taken out. We show that despite the unique synthesis of these complexes, geminal dianions can be described as "extreme" Schrock-type ligands that polarize the metal–carbon bond towards the carbon atom.

## Results and Discussion

**Preparation of an unsymmetrical dilithio methandiide**: In the course of our studies on dilithio methandiides we became interested in the synthesis of unsymmetrically substituted systems.[8,9] So far, almost exclusively symmetric precursors have been used and applied as ligands in carbene complexes. Earlier studies on silyl-substituted systems indicated the somewhat limited flexibility in changing the substitution pattern at the central carbon atom due to the required anion-stabilizing ability.[10,11] Thus, we decided to retain the bis(phosphonium) framework, which has been proven as suitable stabilizing moiety, and to modify the substituents at phosphorus. The starting compound **2** was synthesized from dicyclohexylmethylphosphine sulfide **1**, which was prepared in a one-pot reaction from phosphorus trichloride. Stepwise addition of two equiv of cyclohexylmagnesium chloride followed by methylmagnesium bromide and elemental sulfur afforded **1** as colorless solid in 72% yield (Scheme 1).[12] Deprotonation of the methyl group of **1** with

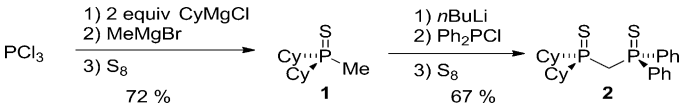


Scheme 1.

*n*-butyllithium was accomplished at room temperature. Subsequent treatment with diphenylchlorophosphine and oxidation with elemental sulfur furnished the bis(thiophosphinoyl)methane **2** as colorless crystalline solid in good yields of 67%. Compound **2** is characterized by a doublet of doublet of the methylene protons in the $^1H$ NMR spectrum and a set of two doublets in the $^{31}P$ NMR spectrum ($\delta_P = 31.4$ and 63.9 ppm, $^2J_{PP} = 18.2$ Hz). The molecular structure of **1** is shown in Figure 2. Compound **1** crystallizes in the ortho-

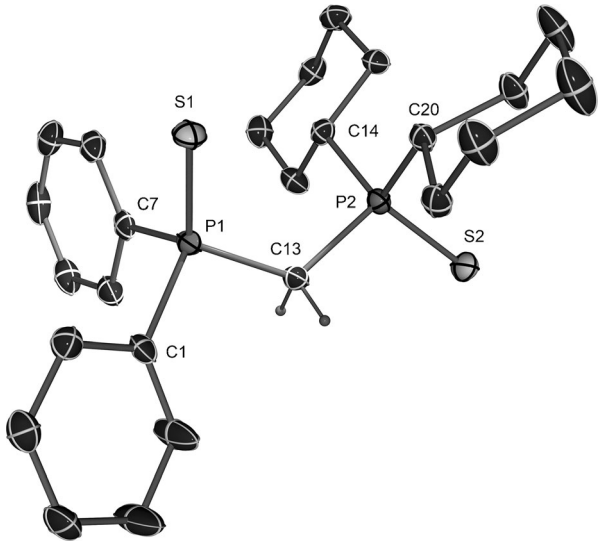


Figure 2. Molecular structure of compound **2**. For crystallographic details see the Supporting Information (thermal ellipsoids at 50% probability level). Selected bond lengths [Å] and angles [°]: C1–P1 1.8272(17), C7–P1 1.8179(17), C14–P2 1.8383(17), C20–P2 1.8366(17), P2–S2 1.964(1), P1–S1 1.951(1), C13–P1 1.841(2), C13–P2 1.841(2), P1-C13-P2 122.6(1), C13-P2-S2 107.5(1), C13-P1-S1 116.9(1).

  

rhombic crystal system, space group $P2_12_12_1$. Both thiophosphinoyl units point to opposite directions in the crystal, thus affording a conformational change for coordination of metals through both sulfur atoms. Bond lengths and angles are in the expected region.

Dimetalation of the methylene unit was first probed in a deuteration experiment (Scheme 2). Treatment of a suspension of the ligand in diethyl ether with methyllithium gave

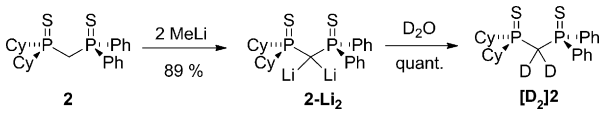


Scheme 2.

way to a clear yellowish solution under gaseous evolution, which was treated with $D_2O$ after 12 h. NMR spectroscopy of the crude product showed the quantitative formation of the bis-deuterated compound, which could be isolated in 97% yield. Compound **[D$_2$]2** is characterized by a broad singlet in the $^2$H NMR spectrum at $\delta = 3.29$ ppm and two multiplets in the $^{31}$P NMR spectrum ($\delta = 31.2$ and 63.7 ppm). For isolation of the intermediate dilithio methandiide, a suspension of **2** in diethyl ether was treated with two equivalents of methyllithium at room temperature. After **2** was completely dissolved, the dilithium salt **2-Li$_2$** starts to crystallize from the reaction mixture as colorless plates and can be isolated in up to 89% yield. Compound **2-Li$_2$** was characterized by multi-nuclear NMR spectroscopy, elemental analysis, and single-crystal X-ray diffraction analysis. The precipitation of **2-Li$_2$** from the reaction mixture is quite surprising as the symmetrical tetraphenyl-substituted derivative is still soluble under these conditions. When introducing the cyclohexyl moieties we expected the contrary tendency. NMR spectroscopy of the dilithio methandiide showed the inclusion of one equivalent of ether in the compound. The $^{31}$P NMR spectrum showed two signals at $\delta = 35.3$ and 55.4 ppm.

The molecular structure of **2-Li$_2$** is depicted in Figure 3. The methandiide crystallizes in the monoclinic crystal system, space group *I*2/a as a highly symmetric dimeric structure, containing only half a molecule in the asymmetric unit, which is assembled to the aggregate through $C_2$ symmetry. In the crystal, the phenyl and cyclohexyl substituents are disordered over the whole molecule with 50% probability for both possible positions. This disorder was found in repeated measurements also when crystals were grown under more dilute conditions and at low temperatures. For refinement, the cyclohexyl substituents were fitted to an ideal model so that no discussion concerning the organic periphery of the structure is possible. Nevertheless, the most interesting part concerns the bonding properties of the S–P–C–P–S (SPCPS) backbone. In total, the structure is similar to the structure reported for the analogue symmetric methandiide.[13] The molecule consists of two dimetalated methandiides and two diethyl ether molecules. The metalated

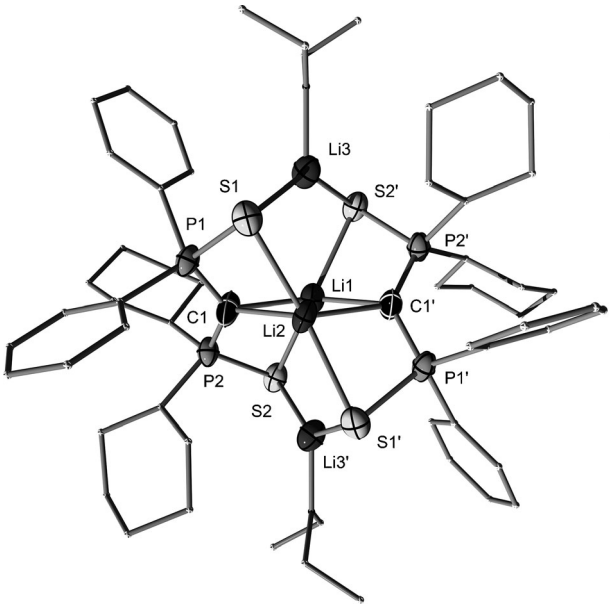


Figure 3. Molecular structure of dilithio methandiide **2**. For crystallographic details see the Supporting Information. Selected bond lengths [Å] and angles [°]: C1–P2 1.676(3), C1–P1 1.681(3), C1–Li2 2.216(6), C1–Li1 2.230(6), Li1–S2 2.484(3), S2–Li3′ 2.405(5), Li2–S1 2.522(2), Li3–O1 1.879(6), Li3–S1 2.395(5), P1–S1 2.039(1), P2–S2 2.035(1); P2-C1-P1 131.4(2), P2-C1-Li2 131.4(2), P1-C1-Li2 92.5(2), P2-C1-Li1 91.3(2), P1-C1-Li1 129.8(2), Li2-C1-Li1 67.6(3), S2′-Li1-S2 144.0(4), S1′-Li2-S1 148.0(4), C1′-Li1-C1 111.9(4).

carbon atom possesses two contacts to the lithium atoms, Li1 and Li2, which lie on the $C_2$ axes of the dimer, thus forming a planar $(CLi)_2$ ring. The two other lithium atoms are solely coordinated by the sulfur atoms of the thiophosphinoyl moieties and diethyl ether. The four lithium atoms form a planar $Li_4$ square with Li–Li distances of 3.262(7) and 3.282(7) Å. The Li–C distances of 2.216(6) and 2.230(6) Å are in the range of oligomeric organolithium compounds.[14]

In the past, it was shown that the double deprotonation of bis(phosphonium)methanes results in a considerable change in the bond lengths of the SPCPS backbone. These changes are also obvious in compound **2-Li$_2$**. The most remarkable changes concern the shortening of the P–C bond lengths by approximately 8% and the elongation of the P–S bond lengths by 4%. Furthermore, a widening of the P-C-P angle from 122.6° in compound **2** to 131.4° in the methandiide is observed. These changes from the neutral to the dianionic compound are in accordance with previous studies on symmetric bis(phosphonium)methandiides[13] and can be referred to the electronic structure, which is best described by a Lewis structure with high charge-separation. Resonance structures with double-bond character have no contribution as also has been found in other methandiides. The charge separation in **2-Li$_2$** results in strong electrostatic interactions within the P–C–P backbone and thus in the contraction of the P–C bonds. Further stabilization of the negative charge at the methanide carbon atom is obtained by negative hyperconjugation into antibonding P–S orbitals, which results

  

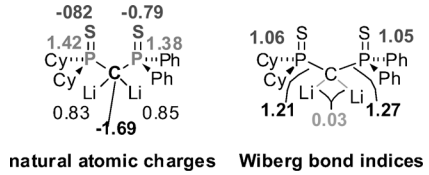


in the lengthening of the respective bonds. This is reflected by the calculated atomic charges and Wiberg bond indices obtained from computational studies of the **2-Li$_2$**.

**Preparation of metal complexes**: The applicability of methandiide **2-Li$_2$** as ligand for transition-metal carbene complexes was tested with zirconocene dichloride as the early transition-metal and (bistriphenylphosphine) palladium chloride as the late transition-metal (Scheme 3). The preparation was accomplished by salt metathesis with one equivalent of [$ZrCl_2Cp_2$] (Cp = cyclopentadienyl) and [$PdCl_2(PPh_3)_2$], respectively.[15] Monitoring of the reaction by using NMR spectroscopy showed the clean formation of the desired complexes. After work-up, the zirconium complex **3** could be isolated by crystallization in 73% yield, and the palladium complex **4** in 63% yield. Both complexes were characterized by multi-nuclear NMR spectroscopy, elemental analysis, and X-ray diffraction analysis.

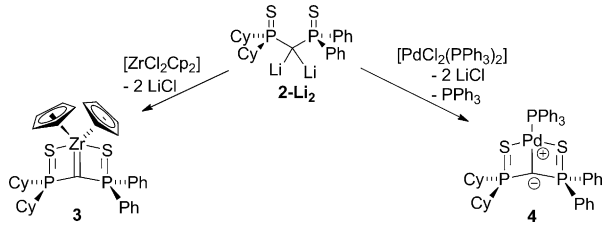


Scheme 3.

The $^{31}P\{^1H\}$ NMR spectrum of **3** features two doublets at $\delta = 20.1$ and 47.8 ppm, which are both upfield-shifted compared with the neutral ligand **2**. In comparison with typical carbene complexes, the carbenic carbon atom resonates at highfield ($\delta = 29.2$ ppm). This has been attributed to the remaining negative charge at the carbon atom and the low double-bond character of the metal–carbon bond (see below).[5b] The coupling constants are considerably larger ($^1J_{CP} = 78.7$ Hz, $^1J_{CP} = 68.8$ Hz) than those found for **2**, which can be attributed to an higher s character of the central carbon atom in the zirconium complex. The $^{31}P\{^1H\}$ NMR spectrum of the palladium complex **4** features three signals of equal intensity. The $PPh_3$ signal resonates at $\delta = 20.8$ ppm as a virtual triplet ($^3J_{PP} = 14.7$ Hz), whereas the phosphorus atoms of the carbene ligand resonate as doublets of doublets at $\delta = 36.6$ ($^2J_{PP} = 33.4$ Hz, $^3J_{PP} = 13.8$ Hz) and 70.1 ppm (dd, $^2J_{PP} = 33.4$ Hz, $^3J_{PP} = 15.5$ Hz). Interestingly, the carbenic carbon atom appears at even higher field than that of complex **3** ($\delta = -18.3$ ppm), which is, to the best of our knowledge, the most shielded carbon-shift compared with related carbene complexes derived from dilithio methandiides. Due to coupling with the adjacent phosphorus atoms the methanide carbon gives rise to an ABX spin system (Figure 4) with $^1J_{CP}$ coupling constants of $^1J_{CP} = 85.0$ and 71.1 Hz.

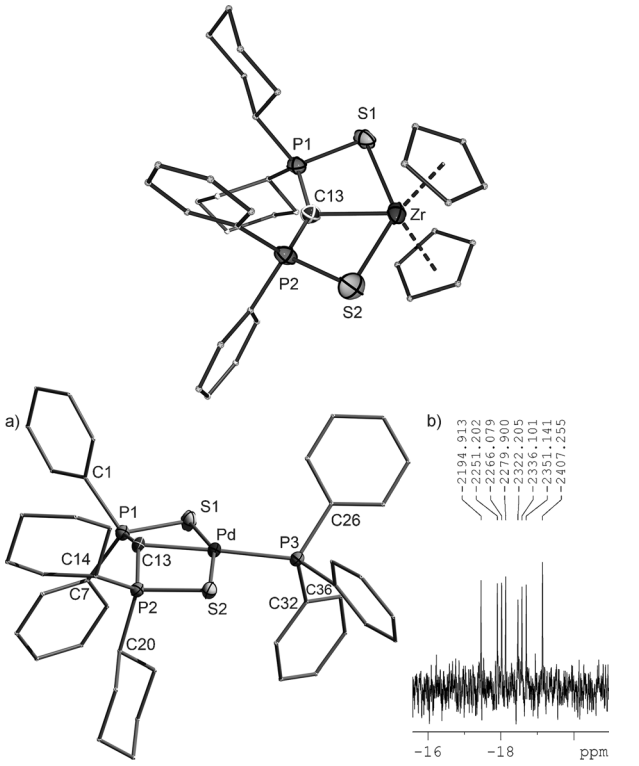


Figure 4. Top: Molecular structure of zirconocene complex **3**. Bottom: a) Molecular structure of palladium complex **4**; b) $^{13}C$ NMR resonance for carbenic carbon in **4**. For crystallographic details see the Supporting Information. Selected bond lengths [Å] and angles [°]: **3**: C1–P1 1.836(2), C7–P1 1.846(2), C13–P2 1.669(2), C13–P1 1.682(2), C14–P2 1.827(2), C20–P2 1.819(2), C13–Zr 2.259(2), P1–S1 2.0297(7), P2–S2 2.0105(8), P2–Zr 3.1508(6), S1–Zr 2.7502(6), S2–Zr 2.7519(7); P2-C13-P1 143.02(12), P2-C13-Zr 105.68(9), P1-C13-Zr 107.87(9), C13-P1-S1 100.40(7), C13-P2-S 103.20(7), P1-S1-Zr1 82.70(2), P2-S2-Zr1 81.23(2). **4**: C13–P1 1.682(3), C13–P2 1.692(3), C13–Pd1 2.101(3), C1–P1 1.822(3), C7–P1 1.820(3), C14–P2 1.831(3), C20–P2 1.842(3), P1–S1 2.040(1), P1–Pd1 2.829(1), P2–S(2) 2.051(1), P2–Pd1 2.802(1), P3–Pd1 2.303(1), Pd1–S2 2.374(1), Pd1–S1 2.388(1); P1-C13-P2 141.3(2), S2-Pd1-S1 158.55(3), C13-Pd1-P3 177.72(7), C13-Pd1-S2 80.13(8), C13-Pd1-S1 80.77(8), P3-Pd1-S1 98.65(3), P3-Pd1-S2 100.05(3).

The molecular structure of the complex **3** and **4** are depicted in Figure 4. Crystal data and structure refinement details are given in the Supporting Information. In accordance with the NMR spectroscopic data, the C–Zr (2.259(2) Å) is rather long and more related to a C–Zr single bond. The methanide carbon atom features a trigonal-planar coordination environment (sum of angles: 356.6(1)°) with C–P distances of 1.682(2) Å to the $PCy_2$ and 1.669(2) Å to the $PPh_2$ moiety. The slightly longer bonds to the cyclohexyl-substituted moiety account for the more electron-rich phosphorus and thus for the less electrostatic attraction with the negatively charged carbon atom. The C–Zr bond however, remains unaffected by the $PCy_2$ substitution.[5b] Overall, the P–C bond lengths are comparable to those found in the di-

  

lithio methandiide **2-Li$_2$** and considerably shortened compared with the neutral ligand **2**, clearly indicating the existing electrostatic interactions within the ligand backbone. This is in line with the elongated P–S bond (2.0297(7) and 2.0105(8) Å) accounting for negative hyperconjugation.

In the molecular structure of **4**, the palladium atom features a distorted square-planar (sum of angles: 350.6°) coordination environment with bond angles between 80.13(8) and 100.05(3)°. The Pd–C distance amounts to 2.101(3) Å, which is slightly shorter than the one reported for the symmetric bis(thiophosphinoyl) ligand (2.113(2) Å), but longer than real Pd–C double bonds.[15] As for the symmetric ligand, complex **4** features a bent coordination mode. Thereby, the PCP backbone arranges almost perpendicularly to the S1–Pd–S2–P3 plane comprising an angle between both planes of 70.0(2)°. Analogous to the zirconocene complex **3**, compound **4** features the same tendencies within the ligand backbone: the P–C bond distances are shorter (1.682(3) and 1.692(3) Å) and the P–S bonds longer (2.051(1) and 2.040(1) Å) than in the free protonated ligand **2**. Due to the unsymmetrical substitution pattern at the carbon atom and its pyramidalization in **4**, the carbon becomes stereogenic. However, in solution, no splitting of the signals (diasterotopic Ph substituents) or broadening was observed.

**DFT calculations: bonding and NMR chemical shifts**: DFT calculations were performed to gain further insight into the electronic structures of **3** and **4** and of related metal-carbene complexes. Structure optimizations were performed on the real systems employing the BP86 functional. The optimized structures are in excellent agreement with the experimental data (see Table S9, the Supporting Information). For comparison, also prototype Fischer complex **A** and Schrock-type complexes **B**–**F** as well as the model systems **G**–**L** were calculated (Figure 6).

Let us first examine the $^{13}$C NMR shifts observed for the carbene carbon atoms, as such parameters have been used previously to discuss donor properties of other carbene ligands, particularly of N-heterocyclic carbenes (NHCs).[16] In the case of carbene complexes derived from dilithio methandiides, a wide range of $^{13}$C NMR shifts (if observed at all) have been reported, with **4** ($\delta = -18.3$ ppm) featuring the most highfield-shifted resonance.[4] Notably, the shifts are in a considerably more shielded region compared with typical Schrock carbene complexes, which typically feature shifts of $\delta = 200$–$400$ ppm.[17] To understand the differences in the $^{13}$C NMR shifts of **3** and **4** relative to each other, to related derivatives, and to more typical Schrock complexes, and to gain further insights into electronic structure, the shifts were computed and analyzed at different computational levels. Table 1 shows results obtained at scalar-relativistic (ZORA-SR) and two-component (ZORA-SO) B3LYP/TZ2P/ZORA/GIAO level in the ADF code, in which the two-component results show the effect of spin-orbit (SO) coupling (NMR shifts obtained at other levels are given in Table S18 in the Supporting Information). SO effects are significantly shielding (about $\delta = -12$ to $-13$ ppm) for **4** but small for **3**. At the two-component level, agreement with experiment may be considered excellent. Already, the importance of spin-orbit effects for **4** shows that a naïve interpretation of the differences in terms of charge is not indicated (indeed, the natural population analysis (NPA) charge on the carbene carbon is more negative in **3**, see Table 2).

Table 1. Comparison of computed and experimental $^{13}$C NMR chemical shifts of the carbine-carbon atoms in **3** and **4** (in ppm vs. TMS).[a]

| $\delta$ $^{13}$C (C carbene) | Exptl | ZORA-SR | ZORA-SO |
|---|---|---|---|
| 3 | 29.2 | 34.7 | 33.1 |
| 4 | −18.3 | −2.2 | −14.8 |

[a] B3LYP/TZ2P/ZORA/GIAO results.

Table 2. Results of the NBO analysis of the carbene complexes **A**–**L**.

| | Charges[a] | | Metal–carbon bond | | | WBI |
|---|---|---|---|---|---|---|
| | $q_C$ | $q_M$ | (occupation) | M [%] | C [%] | |
| **A** | +0.18 | −0.98 | σ (1.91) | 31.52 | 68.48 | 0.84 |
| | | | no π bond | | | |
| **B** | −0.43 | +0.45 | σ (1.95) | 42.39 | 57.61 | 1.70 |
| | | | π (1.70) | 54.27 | 45.73 | |
| **C** | −0.62 | +1.30 | σ (1.97) | 32.08 | 66.82 | 1.82 |
| | | | π (1.94) | 40.17 | 56.98 | |
| **D** | −0.69 | +0.94 | σ (1.98) | 32.15 | 67.75 | 1.68 |
| | | | π (1.87) | 55.87 | 44.01 | |
| **E** | −1.04 | +1.26 | σ (1.94) | 25.72 | 74.28 | 1.82 |
| | | | π (1.90) | 58.96 | 41.04 | |
| **F** | −1.15 | +1.34 | σ (1.96) | 24.72 | 75.18 | 1.63 |
| | | | π (1.90) | 44.57 | 55.35 | |
| **G** | −1.56 | +1.11 | σ (1.86) | 18.95 | 81.05 | 0.72 |
| | | | $LP_C$ (1.57) | – | 100 | |
| **H** | −1.53 | +1.55 | σ (1.81) | 18.04 | 81.96 | 0.67 |
| | | | $LP_C$ (1.57) | – | 100 | |
| **I** | −1.56 | +1.18 | σ (1.86) | 17.40 | 82.60 | 0.68 |
| | | | π (1.73) | 11.93 | 88.07 | |
| **J** | −1.36 | +0.41 | σ (1.87) | 26.92 | 73.08 | 0.89 |
| | | | $LP_C$ (1.50) | – | 100 | |
| **K** | −1.33 | −0.37 | $LP_C$ (1.45) | – | 100 | 0.63 |
| | | | $LP_C$ (1.40) | – | 100 | |
| **L** | −1.32 | +0.28 | σ (1.74) | 39.01 | 60.99 | 0.44 |
| | | | $LP_C$ (1.70) | – | 100 | |

[a] Partial charges of the carbene ligand and the metal center.

Complex **3** exhibits a $\delta = 68$ ppm more shielded value than its homologue, in which the Cp ligands are replaced by chlorine.[4] This is confirmed by computations (see scalar relativistic BP86 results for truncated model complexes **G** and **I** in Table S18, the Supporting Information). These show also that, interestingly, for the simple Schrock-type carbene complexes [Zr(CH$_2$)Cp$_2$] (**F**) and [Zr(CH$_2$)Cl$_2$] (**E**) matters are just reversed for Cp versus Cl ligands.

To understand this better, we have carried out a detailed analysis of the paramagnetic term by breaking it down into individual couplings between (localized) occupied and (canonical) virtual MOs using the IGLO method for the gauge problem (Pipek–Mezey localized MOs have been used, as these are known to provide a separation between σ- and π-

  

orbital manifolds). These detailed analyses for the model complex **I**, its chlorine analogue **G**, and the two abovementioned simple Schrock-type complexes **F** and **E** are given and illustrated in Tables S19–S22 in the Supporting Information (the local MAG/ReSpect program has been used for these analyses, complex **L** is analyzed in Table S23). Here we summarize only the main findings. First of all, the paramagnetic contributions to the isotropic carbene $^{13}C$ shieldings in all four systems are by far dominated by one particularly deshielded component, $\sigma_{11}$, oriented in the carbene plane but perpendicular to the Zr–C bond. Differences between the cyclic complexes **G** and **I** on one side and the classical Schrock complexes **E** and **F** on the other side are also dominated by changes in this component, as are differences between Cp- versus Cl complexes. We may thus concentrate our following discussion on $\sigma_{11}$.

The latter tends to be dominated by contributions from localized molecular orbitals (LMOs) corresponding to a) the Zr–C σ-bond and b) the Zr–C π-bond. More precisely, the former couples to virtual MOs with essentially π*(Zr–C) character, and the latter to virtual MOs with close to σ-antibonding character (Tables S19–S22, the Supporting Information). The visualization of the occupied LMOs indicates both bonds to be evenly distributed over Zr and C for the simple Schrock complexes, whereas the π-bond in the cyclic complexes is essentially a lone pair on the carbene carbon atom. Overall, the much less pronounced deshielding in the cyclic complexes **G** and **I** compared with the classical Schrock complexes **E** and **F** may be attributed both to smaller matrix elements of the relevant perturbation operators (external magnetic field and nuclear magnetic moment), as well as to larger energy denominators.

The $\delta \approx 106$ ppm larger $\sigma_{11}$ component for **I** compared with **G** is largely due to larger energy denominators (Tables S21 and S22, the Supporting Information). That is, the better π-donor ligand Cp raises the low-lying unoccupied MOs on Zr compared with Cl ligands and thereby reduces the paramagnetic terms. Whereas such increased energy denominators are to some extent also present in **F** compared with **E**, here the trend appears to be dominated by increased perturbation matrix elements (Tables S19 and S20, the Supporting Information), consistent with changes in Zr–C covalency (including some involvement of the Cp ligands in the Zr–C σ-bonding LMO and thus the shapes of the relevant orbitals involved. This explains why in this case the chloro complex exhibits an approximately $\delta = 68$ ppm lower carbene $^{13}C$ shift. Additionally, we find that the $\sigma_{22}$ component obtains shielding paramagnetic contributions pointing to off-center ring currents for **G** and **I** (less so for **E** and **F**; see Tables S19–S22). Overall, these analyses indicate a relatively complicated interplay of covalency and energy gaps, thus rendering an understanding without detailed quantum-chemical analysis virtually impossible. Hence, no clear-cut classification of the carbene character in these systems can be made by means of $^{13}C$ NMR shifts.

Therefore, we turned our attention to a detailed study of the bonding situation of the complexes. First, the electronic structure of the Zr and Pd complexes **3** and **4**, respectively, was studied by NBO analyses. Previous studies have shown that carbene complexes based on dilithio methandiides are often characterized by a highly ionic character of the metal–carbon bond. Indeed, NPA charges for **3** and **4** feature a remarkably negative charge on the carbenic carbon atom, which is slightly more pronounced for the zirconium complex (Figure 5). In the case of the metal atom, the palladium

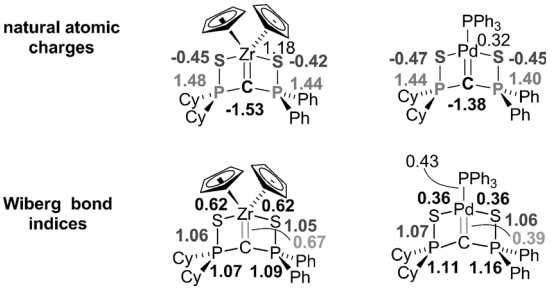


Figure 5. NPA charges and Wiberg bond indices of the complexes **3** and **4**.

atom bears a smaller positive charge compared with the zirconocene complex ($q_{Zr} = +1.14$), which can be considered as a zwitterionic species. This is in line with the calculated Wiberg bond indices of the metal–carbon bonds. Analogous to previous studies, the WBIs were found to be considerably smaller than 1 and thus disagree with a "real", covalent M=C double bond. It is noteworthy, that the NPA charges and Wiberg bond indices are quite similar to those found for the dilithio methandiide **2-Li$_2$** (see above), consistent with the high importance of electrostatic interactions in the ligand backbone.

To better understand the bonding situation in carbene complexes based on dilithio methandiides, we turned our attention to a comparative study of a series of model complexes including the prototype Fischer complex **A** and Schrock-type complexes **B**–**F** (Figure 6). In the case of the dianion-based systems, the complexes **G**–**L** were chosen; they differ in the metal center, the co-ligands, and also the ligand backbone (SCS (**C**) vs. NCN (**D**)). Detailed computational studies by Frenking et al. have revealed unambiguous differences in the bonding situation of Fischer and Schrock complexes in NBO analyses.[18] It was found that the carbene ligands in Schrock complexes carry a distinctly negative partial charge, whereas those in Fischer complexes feature only a small negative or even positive charge. The same tendency (but of opposite direction) was observed for the metal centers. Furthermore it was found, that Schrock complexes always possess metal-carbene σ and π bonds, whereas for Fischer complexes often only the σ-bond is observed. Thereby, the π-electrons in Fischer complexes are polarized towards the metal center, whereas they are more equally distributed in Schrock complexes.[7,18,19] These findings are reflected by the NBO analyses of the prototype Fischer and Schrock complexes **A** and **B**–**F** (Table 2). Considering the

  

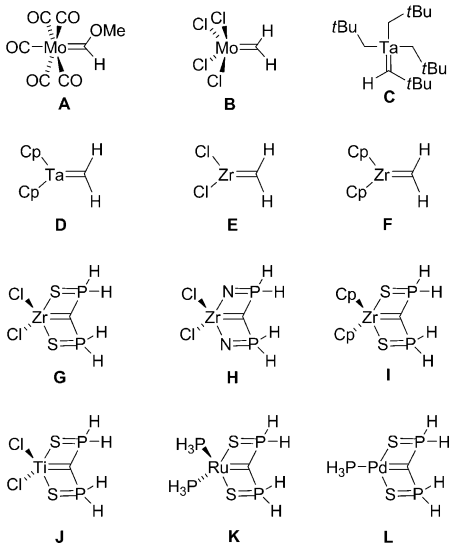


Figure 6. Calculated model complexes.

dianion-based complexes **G**–**L**, the most remarkable feature concerns the charge concentration on the carbenic carbon atom. All compounds, independent of the metal or the co-ligands, feature a high negative charge ($q_C = -1.32$ to $-1.56$). These charges are in general higher than those found in typical Schrock complexes such as **B** ($q_C = -0.43$), but comparable to the hypothetical Schrock complex **F**. Contrary to the charge at the carbon atom, the partial charges of the metal were found to vary strongly, depending on the nature of the metal and the co-ligands. Analogous to the "real" systems **3** and **4** the Wiberg bond indices are significantly smaller than 1, with the smallest value (WBI = 0.44) found for the palladium complex **L**. These values are comparable to the Fischer carbene complex **A** thus indicating a more dative or ionic nature of the metal–carbon bond than normally found in Schrock complexes. Even Schrock complex **F**, with the most pronounced charge separation, features a bond index (WBI = 1.68) that is clearly larger than 1.

Additional information about the metal–carbon bonds in the complexes based on the methandiide ligands is given by the NBOs involved in the bonding (we keep in mind that the NBO Lewis structures do not fully describe the one-particle density matrix in these transition-metal complexes, in particular, when Cp ligands are present). Similar to Fischer carbenes, only a σ-bond is observed for most of the examples **G**–**L**. These bonds are clearly polarized towards the carbon end (e.g., 83% in **I**). Furthermore, the complexes **G**–**L** generally feature an additional lone pair (LP) at the carbene carbon, which is in line with the high negative partial charge at the carbene ligand and the usually observed nucleophilic character. In contrast to this picture, all calculated Schrock complexes possess metal-carbene σ and π bonds as reported earlier.[18,20] This is also the case for the more polarized complex **F**, which is (in terms of charges) the system best comparable with the complexes based on the methandiide ligands. Notably, complex **I** exhibits a larger negative charge on the carbene carbon atom than **L**, in spite of the fact that the Zr $d^0$ center in the latter may function as a π-acceptor, whereas the Pd $d^8$ center in **L** may not. This reflects the lower electronegativity of Zr (mainly in the σ bond).[21]

The bonding situation obtained from the NBO analyses is well reflected by the canonical molecular orbitals of these compounds. Figure 7 exemplarily depicts the important molecular orbitals for the Schrock-type complex **B** and the titanium complex **J**. Overall, these data show that carbene complexes based on dilithio methandiides are formally Schrock-type ligands, however with a stronger polarization and no truly covalent nature of the metal–carbon bond. In comparison to the prototype Schrock complexes such as **B**, which are best described by a classical M=C double bond (resonance structure **cov**, Figure 7), these ligands favor the more ionic resonance structure **ion** with a metal–carbon single bond and a remaining lone pair at the carbon. It should be noted that this ionic formulation is often used in textbooks to explain the nucleophilic nature of Schrock complexes.[22] This leads us to conclude that geminal dianions are a kind of "extreme" Schrock-type ligands. However, one has to keep in mind that the metal–carbon interaction also depends on the nature of the metal center. Thus, interactions between the two extreme canonical forms M=C and $M^{2+}\cdots C^{2-}$ are possible. So far, the most "covalent" interactions are hitherto observed for uranium complexes of methandiides with bond indices in the range of archetypal Schrock complexes.[23] We would like to point out that the methandiide-based systems presented in this manuscript do not fulfill the criterion of M=C double-bonded systems. In the case of the palladium complexes **4** or **L**, the complexes are actually

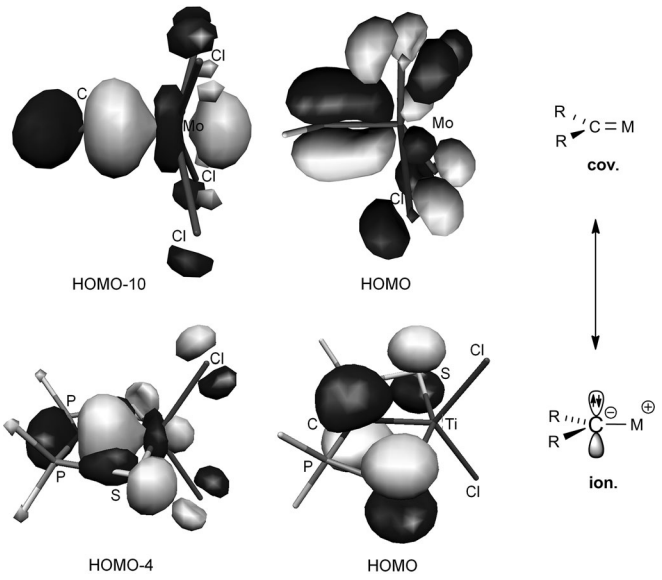


Figure 7. Top: Molecular orbitals of Schrock complex **B**. Bottom: Titanium complex **I** (isosurface value at 0.05).

  

better described as masked methandiides with the totally ionic resonance structure $M^{2+}\cdots C^{2-}$.

Table S26 in the Supporting Information also provides a graphical comparison of the electron localization function (ELF; see the Computational Details) for compounds **3**, **4**, and for the Schrock model complex **F**. The ELF confirms the relatively localized π-type carbon lone-pair in **3**, a more asymmetrical one in **4**, and the involvement of the corresponding orbitals in covalent Zr–C π-bonding in the Schrock complex **F**. A similar picture is obtained from the AIM studies.[24] Table 3 gives selected results of the topological analysis of some of the complexes. The ellipticity $\varepsilon$ of the electron density at the $M-C_{carbene}$ bond critical point (BCP) is the most significant property, as it provides a measure of the double-bond character in the carbene complexes. Cylindrically symmetrical σ bonds are characterized by an ellipticity value close to zero, whereas the presence of one π-bond gives rise to nonzero ellipticities. This is seen nicely for the Schrock complexes **E** and **F** ($\varepsilon > 0$), thus confirming the π-bonding interaction.[18] For the methandiide-based complexes significantly smaller ellipticities are calculated, corroborating the small role of M–C π-interactions in these compounds.[25] This is particularly true for the palladium complexes **L** and **4**, which feature typical values of purely σ-bonded systems.

Table 3. Bond critical point (BCP) properties for the M–C carbene bond.

| | $\rho_{BCP}$ [a.u.] | $\nabla^2\rho$ [a.u.] | $\varepsilon$ [a.u.] |
|---|---|---|---|
| **E** | 0.153 | 0.159 | 0.62 |
| **F** | 0.128 | 0.173 | 0.54 |
| **H** | 0.095 | 0.134 | 0.28 |
| **I** | 0.084 | 0.135 | 0.21 |
| **3** | 0.067 | 0.131 | 0.21 |
| **L** | 0.108 | 0.128 | 0.02 |
| **4** | 0.106 | 0.124 | 0.03 |

[a] Electron density ($\rho_{BCP}$), Laplacian ($\nabla 2\rho$), and ellipticity ($\varepsilon$).

## Conclusion

We present the synthesis of a new unsymmetrical geminal dianion and its application as ligand in zirconium- and palladium-carbene complexes. Both complexes were found to exhibit extremely shielded $^{13}C$ NMR shifts, which are even more highfield-shifted than those of related carbene complexes based on dilithio methandiides. DFT analyses indicate significant spin-orbit effects for the palladium complex. But mostly the lower shifts of both Zr and Pd complexes compared with standard Schrock carbene complexes may be attributed to a combination of 1) smaller relevant energy denominators and 2) more delocalized and polar Zr–C bonding.

The electronic structure of these and related complexes has been compared to typical Fischer and Schrock complexes. Charge separation in the metal–carbon bond is comparable but yet more pronounced than in typical Schrock systems underlining the overall nucleophilic character of both classes of compounds. However, bond orders were found to be significantly lower than in the Schrock complexes and in most of the cases the π-bonds are strongly polarized to carbon (or truly absent for the Pd complex). Carbene complexes based on dilithio methandiides may thus be viewed formally as Schrock-type systems, but with a more pronounced ionic nature of the metal–carbon bond. This leads to the conclusion that geminal dianions represent a kind of "extreme" Schrock-type ligands often favoring the ionic resonance structure $M^{+}-CR_2^{-}$ as used to in textbooks to explain the nucleophilic nature of Schrock complexes. In some cases the totally ionic structure $M^{2+}\cdots C^{2-}$ is even a more realistic description (i.e., masked dianion). Nevertheless, geminal dianions provide a unique strategy to access Schrock-like complexes, also allowing the introduction of late transition-metals. It will be interesting to see whether also other methandiides than bis(phosphonium)-substituted systems can be applied in the synthesis of the corresponding carbene complexes. By the use of less anion-stabilizing moieties, a more covalent metal–carbon interaction and thus more "classical" Schrock complexes should be realizable.

## Experimental Section

**General procedures**: All experiments were carried out under a dry, oxygen-free argon atmosphere by using standard Schlenk techniques. Involved solvents were dried over sodium or potassium and distilled prior to use. $H_2O$ is distilled water. Organolithium reagents were titrated against diphenylacetic acid prior use. $^1H$, $^{13}C$, $^{31}P$ NMR spectra were recorded on Avance-500 or AMX-400 Bruker spectrometers at 22 °C if not stated otherwise. All values of the chemical shift are in ppm regarding the $\delta$ scale. All spin-spin coupling constants ($J$) are printed in Hertz (Hz). To display multiplicities and signal forms correctly the following abbreviations were used: s = singlet, d = doublet, t = triplet, q = quartet, m = multiplet, br = broad signal. GC/MS analyses were performed on a Varian 320MS-GC/MS. Diphenylchlorophosphine, cyclohexylmagnesium chloride, bis(triphenylphosphine)palladium dichloride, zirconocene dichloride were purchased and used without further purification.

**One-pot synthesis of compound 1**: In a 500 mL Schlenk flask posphorus trichloride (4.08 g, 29.7 mmol) was dissolved in THF (80 mL). Under vigorous stirring cyclohexylmagnesium chloride ((30 mL, 60.0 mmol; 3 M solution in diethyl ether) were slowly added at −78 °C resulting in the precipitation of magnesium chloride. After 5 h at room temperature the solvent was partly removed in vacuo and pentane (60 mL) was added. The mixture was filtered by cannula transfer and the remaining solid washed twice with additional pentane (40 mL). Subsequently, THF (40 mL) were added to the solution followed by the addition of methylmagnesium bromide (12 mL, 23.0 mmol; 3 M solution in diethyl ether) at −78 °C. The mixture was allowed to warm to RT and stirred overnight. Then, elemental sulfur (1.28 g, 40.0 mmol) was added and the mixture stirred for additional 3 h. The yellow solution was treated with water (50 mL) and the mixture extracted with diethyl ether. The combined organic layers were dried over sodium sulfate and the solvent removed in vacuo giving a yellow solid. Purification by sublimation by using Kugelrohr distillation (132–137 °C, $1\times10^{-3}$ mbar) afforded the product as colorless solid in 72% yield (5.21 g, 21.3 mmol). The spectroscopic data matches the published data.[26]

**Synthesis of 2**: *n*-butyllithium (4.10 mL, 6.57 mmol, 1.6 M solution in hexane) was added to a cooled solution of 1.60 g (6.57 mmol) of **1** in THF (40 mL) giving an orange-colored solution. After stirring for 2 h at RT the mixture was again cooled to −78 °C and slowly added to a solution of diphenylchlorophosphine (1.68 g, 7.00 mmol) in diethyl ether (60 mL). The solution was allowed to warm to RT and stirred overnight. Subsequently, elemental sulfur (0.22 g, 7.00 mmol) was added and the mixture stirred for 3 h at RT. After the addition of water (50 mL) the mixture was extracted with diethyl ether. The combined organic layers were dried over sodium sulfate and the solvent removed in vacuo giving a yellow oil. Purification by flash chromatography on silica (eluent: pentane/diethylether: v/v = 2:1) gave the product as a colorless solid in 67 % yield (2.03g, 4.40 mmol). $R_f$ = 0.6; $^1$H NMR (500 MHz, $CDCl_3$): $\delta$ = 1.02–1.12 (m, 6H, C$H_2$,cyclohexyl), 1.38–1.44 (m, 4H; C$H_2$,cyclohexyl), 1.59–1.87 (m, 10H; C$H_2$,cyclohexyl), 2.40–2.43 (m, 2H; C$H$P), 3.31 (dd, $^2J_{HP}$ = 13.8 Hz, $^2J_{HP}$ = 12.1 Hz, 2H; PC$H_2$P), 7.46-7.52 (m, 6H; C$H_{Ph,meta,para}$), 7.90–7.93 ppm (m, 4H; C$H_{Ph,ortho}$); $^{13}$C NMR (125.8 MHz, $CDCl_3$): $\delta$ = 25.4 (d, $^4J_{CP}$ = 1.71 Hz, PCH($CH_2CH_2$)$_2CH_2$), 26.0 (d, $J_{CP}$ = 7.18 Hz; $CH_2$), 26.1 (d, $J_{CP}$ = 7.51 Hz; $CH_2$), 26.6 (d, $J_{CP}$ = 2.60 Hz; $CH_2$), 26.7 (d, $J_{CP}$ = 3.41 Hz; $CH_2$), 32.8 (dd, $^1J_{CP}$ = 39.8 Hz, $^1J_{CP}$ = 31.1 Hz; P$CH_2$P), 37.8 (d, $^1J_{CP}$ = 47.3 Hz; P$CH$), 128.7 (d, $^3J_{CP}$ = 12.5 Hz; C$H_{meta}$), 129.9 (d, $^2J_{CP}$ = 10.6 Hz, C$H_{ortho}$), 131.8 (d, $^4J_{CP}$ = 3.02 Hz; C$H_{para}$), 133.4 ppm (dd, $^1J_{CP}$ = 82.2 Hz, $^3J_{CP}$ = 2.44 Hz, P$C_{ipso}$); $^{31}$P NMR (162.0 MHz, $CDCl_3$): $\delta$ = 31.4 (d, $^2J_{PP}$ = 18.2 Hz; $P$Ph$_2$), 63.9 ppm (d, $^2J_{PP}$ = 18.2 Hz; $P$Cy$_2$); elemental analysis calcd (%) for $C_{25}H_{34}P_2S_2$: C, 65.19; H, 7.44; S 13.92; found: C, 65.30; H, 7.56; S 13.72.

**Synthesis of [D$_2$]2**: Compound **2** (200 mg, 0.43 mmol) was suspended in diethyl ether (10 mL) and cooled to −30 °C. Methyllithium (0.56 mL, 0.88 mmol; 1.58 M in diethylether) was added upon which the solid fully dissolved under gaseous evolution. The yellowish solution was stirred for 12 h and subsequently $D_2O$ (3 mL) were added. After 2 h stirring at room temperature, the mixture was extracted with diethyl ether (3 × 10 mL), the combined organic layers dried over sodium sulfate and the solvent removed in vacuo. The obtained solid was subsequently purified via column chromatography (pentane/$Et_2O$ = 2:1) giving the product as colorless solid (192 mg, 42 mmol; 97 %). $^1$H NMR (500 MHz, $CDCl_3$): $\delta$ = 1.02–1.12 (m, 6H, C$H_2$,cyclohexyl), 1.38-1.42 (m, 4H; C$H_2$, cyclohexyl), 1.58–1.89 (m, 10H; C$H_2$,cyclohexyl), 2.40–2.43 (m, 2H; C$H$P), 7.45–7.50 (m, 6H; C$H_{Ph,meta,para}$), 7.90–7.95 ppm (m, 4H; C$H_{Ph,ortho}$); $^2$H NMR (76.8 MHz, $CDCl_3$): $\delta$ = 3.29 ppm (br); $^{13}$C NMR (125.8, $CDCl_3$): $\delta$ = 25.4 (d, $^4J_{CP}$ = 1.70 Hz, PCH($CH_2CH_2$)$_2CH_2$), 26.0 (d, $J_{CP}$ = 7.29 Hz; PCH-($CH_2CH_2$)$_2CH_2$), 26.1 (d, $J_{CP}$ = 7.60 Hz; PCH($CH_2CH_2$)$_2CH_2$), 26.6 (d, $J_{CP}$ = 2.57 Hz; PCH$CH_2$), 26.7 (d, $J_{CP}$ = 3.36 Hz; PCH$CH_2$), 32.4 (br; P$CD_2$P), 37.8 (m; P$CH$), 128.7 (d, $^3J_{CP}$ = 12.5 Hz; C$H_{meta}$), 129.9 (d, $^2J_{CP}$ = 10.6 Hz, C$H_{ortho}$), 131.8 (d, $^4J_{CP}$ = 3.03 Hz; C$H_{para}$), 133.4 ppm (dd, $^1J_{CP}$ = 82.1 Hz, $^3J_{CP}$ = 2.47 Hz, P$C_{ipso}$); $^{31}$P NMR (162.0 MHz, $CDCl_3$): $\delta$ = 31.2 (m; $P$Ph$_2$), 63.7 (m; $P$Cy$_2$); elemental analysis calcd (%) for $C_{25}H_{34}P_2S_2$: C, 64.90; H, 7.84; S 13.86; found: C, 64.83; H, 7.48; S 13.78.

**Synthesis of 2-Li$_2$**: Compound **2** (100 mg, 0.23 mmol) was suspended in diethyl ether (5 mL). Methyllithium (0.32 mL, 0.50 mmol; 1.56 M in diethyl ether) was then added giving a yellow solution. Under gaseous evolution the solid completely dissolved and the product started to crystallize out of the reaction mixture. After 18 h at RT, the remaining solution was removed and the crystalline solid dried in vacuo giving the product as colorless solid in 80–89 % yield. $^1$H NMR: (400.1 MHz, $C_6D_6$): $\delta$ = 1.52–2.25 (m, 20H; C$H_{2Cy}$), 3.23–3.28 (m, 2H; C$H_{Cy}$), 7.02–7.21 (m, 6H; C$H_{PH,meta/para}$), 8.18–8.23 ppm (m, 4H; C$H_{Ph,ortho}$); $^7$Li NMR (155.5 MHz, $C_6D_6$): $\delta$ = 1.9; $^{31}$P NMR (162.0 MHz, $C_6D_6$): $\delta$ = 35.3 ($P$Ph$_2$), 55.4 ppm ($P$Cy$_2$). Solubility too low in benzene, toluene and THF to obtain $^{13}$C NMR data; elemental analysis calcd (%) for $C_{49}H_{52}Li_2OP_2S_2$: C, 63.72; H, 7.74; S 11.73; found: C, 63.46; H, 8.03; S 11.50.

**Synthesis of complex 3**: Zirconocene dichloride (80 mg, 0.27 mmol) was dissolved in tetrahydrofurane and added to a suspension of dilithium salt **1** (150 mg, 0.27 mmol) in toluene. The suspension was stirred at room temperature for 20 h, upon which the solution turned yellow and all solids completely dissolved. After removal of the solvent in vacuo the residue was taken up in toluene and filtered to remove lithium chloride. After reduction of the solvent to about 1 mL, the product started to crystallize out of the reaction mixture and was isolated as yellow solid after removal of the remaining solution (139 mg, 0.20 mmol; 73 %). $^1$H NMR (400 MHz, $C_6D_6$): $\delta$ = 0.93–0.97 (m, 2H, C$H_{2,Cy}$), 1.09–1.22 (m, 4H, C$H_{2,Cy}$), 1.39–1.42 (m, 2H; C$H_{2,Cy}$), 1.55–1.62 (m, 4H, C$H_{2,Cy}$), 1.70–1.82 (m, 8H; C$H_{2,Cy}$), 2.13-2.14 (m, 2H; C$H$P), 6.31 (d, 10H; C$H_{Cp}$), 7.16–7.21 (m, 6H; C$H_{Ph,meta,para}$), 7.96–8.02 ppm (m, 4H; C$H_{Ph,ortho}$); $^{13}$C NMR (100.6, $C_6D_6$): $\delta$ = 26.1 (d, $J_{CP}$ = 2.36 Hz; C$H_{2,Cy}$), 26.2 (d, $J_{CP}$ = 1.68 Hz; C$H_{2,Cy}$), 26.6 (d, $J_{CP}$ = 1.75 Hz; C$H_{2,Cy}$), 26.9 (d, $^2J_{CP}$ = 5.30 Hz C$H_{2,Cy}$), 27.1 (d, $^2J_{CP}$ = 5.87 Hz; C$H_{2,Cy}$), 29.2 (dd, $^1J_{CP}$ = 78.7 Hz, $^1J_{CP}$ = 68.8 Hz; P$C$P), 42.8 (dd,$^1J_{CP}$ = 42.0 Hz, $^3J_{CP}$ = 1.33 Hz; P$C$H), 112.8 ($C_{Cp}$), 128.3 (d, $^3J_{CP}$ = 11.5 Hz; C$H_{meta}$), 130.1 (d, $^4J_{CP}$ = 2.90 Hz; C$H_{para}$), 130.6 (d, $^2J_{CP}$ = 11.6 Hz, C$H_{ortho}$), 141.3 ppm (dd, $^1J_{CP}$ = 69.9 Hz, $^3J_{CP}$ = 1.65 Hz, P$C_{ipso}$); $^{31}$P NMR (162.0 MHz, $C_6D_6$): $\delta$ = 20.1 (d, $^2J_{PP}$ = 3.30 Hz; $P$Ph$_2$), 47.8 ppm (d, $^2J_{PP}$ = 3.30 Hz, $P$Cy$_2$); elemental analysis calcd (%) for $C_{37}H_{48}P_2S_2Zr$: C, 62.58; H, 6.81; S 9.03; found: C, 62.17; H, 6.49; S 8.95.

**Synthesis of complex 4**: Dianion (90 mg, 0.16 mmol) and bis(triphenylphosphine)palladium dichloride (112 mg, 0.16 mmol) were suspended in toluene (10 mL) and stirred for 3 d at RT. The obtained red suspension was filtered through a filter cannula and the solvent removed in vacuo to afford a red solid. The residue was taken up in toluene (8 mL) and the solvent reduced to about 2 mL, from which the complex started to precipitate. The remaining solvent was removed, the solid washed three times with pentane/diethyl ether (v/v = 1:1) and dried in vacuo giving the product as red solid (83 mg, 0.10 mmol; 63 %). $^1$H NMR (400 MHz, $CD_2Cl_2$): $\delta$ = 0.90-1.18 (m, 6H, C$H_{2,Cy}$), 1.34–1.54 (m, 6H, C$H_{2,Cy}$), 1.58–1.69 (m, 4H; C$H_{2,Cy}$), 1.70–1.80 (m, 4H, C$H_{2,Cy}$), 1.90–2.02 (m, 2H; C$H$P), 7.28-7.46 (m, 15H; C$H_{Ph,meta,para}$), 7.53–7.58 (m, 4H; C$H_{PPh3,ortho}$), 7.69–7.75 ppm (m, 4H; C$H_{PPh2,ortho}$); $^{13}$C NMR (125.8, $CD_2Cl_2$): $\delta$ = −18.3 (ddd, $^1J_{CP}$ = 85.0 Hz, $^1J_{CP}$ = 71.1 Hz, $^2J_{CP}$ = 56.1 Hz; P$C$P), 26.1 (m; C$H_{2,Cy}$), 26.4 (d, $^2J_{CP}$ = 1.66 Hz; C$H_{2,Cy}$), 26.7 (d, $^2J_{CP}$ = 6.66 Hz; C$H_{2,Cy}$), 26.8 (d, $^2J_{CP}$ = 7.26 Hz C$H_{2,Cy}$), 41.6 (dd,$^1J_{CP}$ = 41.9 Hz, $^3J_{CP}$ = 2.13 Hz; P$CH$), 128.5 (d, $^3J_{CP}$ = 11.4 Hz; C$H_{PPh2,meta}$), 128.6 (d, $^3J_{CP}$ = 11.5 Hz; C$H_{PPh3,meta}$), 130.0 (d, $^2J_{CP}$ = 11.8 Hz, C$H_{PPh2,ortho}$), 130.2 (d, $^4J_{CP}$ = 2.00 Hz; C$H_{PPh3,para}$), 130.9 (d, $^4J_{CP}$ = 3.02 Hz; C$H_{PPh2,para}$), 133.1 (d, $^1J_{CP}$ = 35.1 Hz; P$C_{PPh3,ipso}$), 134.6 (d, $^2J_{CP}$ = 12.6 Hz, C$H_{PPh3,ortho}$), 141.2 ppm (ddd, $^1J_{CP}$ = 72.2 Hz, $^3J_{CP}$ = 3.04 Hz, $^4J_{CP}$ = 1.52 Hz; P$C_{PPh2,ipso}$); $^{31}$P NMR (162.0 MHz, $CD_2Cl_2$): $\delta$ = 20.8 (vt, $^3J_{PP}$ = 14.7 Hz; $P$Ph$_3$), 36.6 (dd, $^2J_{PP}$ = 33.4 Hz, $^3J_{PP}$ = 13.8 Hz; $P$Ph$_2$), 70.1 ppm (dd, $^2J_{PP}$ = 33.4 Hz, $^3J_{PP}$ = 15.5 Hz; $P$Cy$_2$); $^{31}$P NMR (162.0 MHz, $C_6D_6$): $\delta$ = 35.3 (t, $^2J_{PP}$ = 15.9 Hz, $^2J_{PP}$ = 30.0 Hz; PPh$_3$), 36.3 (dd, $^2J_{PP}$ = 14.2 Hz, $^2J_{PP}$ = 38.8 Hz; PPh$_2$), 68.3 ppm (dd, $^2J_{PP}$ = 15.8 Hz, $^2J_{PP}$ = 38.8 Hz; PCy$_2$); elemental analysis calcd (%) for $C_{43}H_{47}P_3S_2Pd$: C, 62.43; H, 5.73; S 7.75; found: C, 61.99; H, 5.71; S 7.42.

**Single-crystal X-ray structure determination**: Single crystals were selected from a Schlenk flask under an argon atmosphere and covered with inert oil (perfluoropolyalkylether). Data for compounds **2** and **2-Li$_2$** were collected on a Bruker X8Apex diffractometer, data for **3** and **4** were collected on Bruker APEX-CCD (D8 three-circle goniometer) (Bruker AXS). Integration was conducted with SAINT and an empirical absorption correction (SADABS) was applied. The structures were solved by direct (**2**, **2-Li$_2$**, **3** and **4**) methods (SHELXS-97) and refined by full-matrix least-squares methods against F2 (SHELX$_L$-97).[27] All non-hydrogen atoms were refined with anisotropic displacement parameters. Hydrogen atoms were placed in calculated positions and refined using the riding model. Relevant details about the structure refinements are given Tables S1–S10 (the Supporting Information). CCDC-965733 (**2**) and CCDC-965734 (**2-Li$_2$**) CCDC-965735 (**3**), and CCDC-965736 (**4**) contain the supplementary crystallographic data for this paper. These data can be obtained free of charge from The Cambridge Crystallographic Data Centre via www.ccdc.cam.ac.uk/data_request/cif.

*Crystal data for* **2**: $C_{25}H_{34}P_2S_2$; $M_r$ = 460.58; colorless block; 0.35 × 0.28 × 0.24 mm$^3$; orthorhombic; space group $P2_12_12_1$; $a$ = 9.6725(4), $b$ = 12.4667(5), $c$ = 20.2529(7) Å; $V$ = 2442.18(16) Å$^3$; $Z$ = 4; $\rho_{calcd}$ = 1.253 gcm$^{-3}$; $\mu$ = 0.359 mm$^{-1}$; $F(000)$ = 984; $T$ = 100(2) K; $R_1$ = 0.0246 and $wR^2$ = 0.0560; 4280 unique reflections ($\theta$ < 24.99) and 262 parameters.

*Crystal data for* **2-Li$_2$**: $C_{58}H_{84}Li_4O_2P_4S_4$; $M_r$ = 1093.13; colorless plate; 0.21 × 0.21 × 0.06 mm$^3$; monoclinic; space group $I2/a$; $a$ = 16.9670(12), $b$ = 13.0321(9), $c$ = 28.097(2) Å; $\beta$ = 106.860(4) °; $V$ = 5945.7(8) Å$^3$; $Z$ = 4; $\rho_{calcd}$ = 1.221 gcm$^{-3}$; $\mu$ = 0.307 mm$^{-1}$; $F(000)$ = 2336; $T$ = 100(2) K; $R_1$ =

  

0.0492 and $wR^2 = 0.1256$; 5236 unique reflections ($\theta < 25.00$) and 478 parameters.

*Crystal data for* **3**: $C_{35}H_{42}P_2S_2Zr$; $M_r = 679.97$; yellow block; $0.31 \times 0.21 \times 0.17\ mm^3$; triclinic; space group $P\bar{1}$; $a = 10.1685(11)$, $b = 11.8680(13)$, $c = 13.4916(15)$ Å; $\alpha = 93.889(2)$, $\beta = 96.726(2)$, $\gamma = 91.096(2)°$; $V = 1612.6(3)$ Å$^3$; $Z = 2$; $\rho_{calcd} = 1.400\ g cm^{-3}$; $\mu = 0.593\ mm^{-1}$; $F(000) = 708$; $T = 173(2)$ K; $R_1 = 0.0275$ and $wR^2 = 0.0715$; 5664 unique reflections ($\theta < 25.00$) and 361 parameters.

*Crystal data for* **4**: $C_{43}H_{47}P_3PdS_2$; $M_r = 827.24$; red plate; $0.21 \times 0.18 \times 0.09\ mm^3$; triclinic; space group $P\bar{1}$; $a = 9.5630(19)$, $b = 14.231(3)$, $c = 14.758(3)$ Å; $\alpha = 93.09(3)$, $\beta = 100.56(3)$, $\gamma = 98.48(3)°$; $V = 1946.1(7)$ Å$^3$; $Z = 2$; $\rho_{calcd} = 1.412\ g cm^{-3}$; $\mu = 0.738\ mm^{-1}$; $F(000) = 856$; $T = 173(2)$ K; $R_1 = 0.0286$ and $wR^2 = 0.0771$; 6858 unique reflections ($\theta < 25.00$) and 442 parameters.

**Computational details**: All calculations (except for **2-Li$_2$**, $C_2$ symmetry) were performed without symmetry restrictions. Starting coordinates were obtained directly from the crystal structure analyses. All calculations were done with the Gaussian 03 (Revision E.01) program package.[28a] Structure optimizations were performed at the density-functional theory level using the Becke–Perdew (BP86) functional.[29] The 6-31+G* basis set was used for hydrogen, carbon, and lithium, the 6-311+G** basis set for all other atoms (P, S). For palladium and zirconium the LANL2TZ(f)[30] basis set of triple-ζ quality was used augmented with an f polarization function of exponent 1.472 and 0.875, respectively.[31] Harmonic vibrational frequency analyses were performed at the same levels of theory to confirm that the structures were indeed minima on the potential energy surface (PES). NBO analyses were carried out on the optimized systems using the NBO 5.G program,[28b] interfaced to the Gaussian 03 program. The wave functions were also analyzed in DGrid[32] program by means of the electron localization function (ELF)[33] and the quantum theory of atoms in molecules (AIM).[24] For this purpose, the Kohn–Sham orbitals of the single point calculations were transferred to the DGrid and the examined property was calculated on a grid with 50 points per Bohr. The ELF results were visualized in selected planes using the standard ELF color scale and the Paraview program.[34]

Quasirelativistic all-electron DFT calculations of the nuclear shieldings have been performed using the Amsterdam Density Functional (ADF)[35] program suite, employing Slater-type orbital (STO) basis sets of triple-zeta doubly polarized (TZ2P) quality and the B3LYP[36] functional. Both scalar and SO relativistic effects were treated by the two-component zero-order regular approximation (ZORA).[37] Gauge-including atomic orbitals (GIAOs)[38] were used. The computed $^{13}C$ nuclear shieldings were converted into chemical shifts ($\delta$, in ppm) relative to the shielding of tetramethylsilane (TMS), obtained at the same computational level.

Analyses of the nuclear shielding constants in model complexes were carried out separately, in two steps: first the restricted Kohn–Sham orbitals were generated with the Gaussian 09[39] program package, using the BP86[40] functional. For Zr and Pd, a quasi-relativistic energy-adjusted small-core Stuttgart-type pseudopotential (effective-core potential, ECP) with corresponding (8s7p6d)/[6s5p3d] GTO valence basis set was used.[41] Ligand atoms were treated by Huzinaga–Kutzelnigg-type IGLO-III basis sets.[41] Subsequently, the Kohn–Sham orbitals were transferred to the MAG-ReSpect[42] property package by interface routines. The nuclear shielding constants were calculated either by using independent gauges for localized molecular orbitals (IGLO)[41] in combination with a Pipek-Mezey[43] localization procedure (together with an excitation analysis as implemented in MAG-ReSpect program package) or at GIAO level. The visualization of localized and canonical molecular orbitals was done with Molekel.[44]

## Acknowledgements

V.H.G. acknowledges the Deutsche Forschungsgemeinschaft for an Emmy-Noether grant (DA-1402/1-1) as well as the Fonds der Chemischen Industrie, the Alexander von Humboldt Foundation and the University of Würzburg for financial support. Work in Berlin was funded by the DFG excellence cluster on "Unifying concepts in catalysis" (UniCat). We also thank Rockwood Lithium for the supply of chemicals.

[1] a) U. Klabunde, E. O. Fischer, *J. Am. Chem. Soc.* **1967**, *89*, 7141–7142; b) R. R. Schrock, *J. Am. Chem. Soc.* **1974**, *96*, 6796–6797.

[2] For reviews, see: a) N. D. Jones, R. G. Cavell, *J. Organomet. Chem.* **2005**, *690*, 5485–5496; b) T. Cantat, N. Mézailles, A. Auffrant, P. Le Floch, *Dalton Trans.* **2008**, 1957–1972; c) S. T. Liddle, D. P. Mills, A. Wooles, *J. Organomet. Chem.* **2010**, *36*, 29; d) S. Harder, *Coord. Chem. Rev.* **2011**, *255*, 1252; e) T. K. Panda, P. W. Roesky, *Chem. Soc. Rev.* **2009**, *38*, 2782–2804; f) S. T. Liddle, D. P. Mills, A. J. Wooles, *Chem. Soc. Rev.* **2011**, *40*, 2164–2176; g) G. R. Giesbrecht, J. C. Gordon, *Dalton Trans.* **2004**, 2387–2393; h) O. T. Summerscales, J. C. Gordon, *RSC Adv.* **2013**, *3*, 6682–6692.

[3] D. J. Mindiola, J. Scott, *Nat. Chem.* **2011**, *3*, 15–17.

[4] For examples, see: a) R. P. K. Babu, R. McDonald, S. A. Decker, M. Klobukowski, R. G. Cavell, *Organometallics* **1999**, *18*, 4226–4229; b) O. J. Cooper, D. P. Mills, J. McMaster, F. Moro, E. S. Davies, W. Lewis, A. J. Blake, S. T. Liddle, *Angew. Chem.* **2011**, *123*, 2431–2434; *Angew. Chem. Int. Ed.* **2011**, *50*, 2383–2386; c) R. G. Cavell, R. P. K. Babu, A. Kasani, R. McDonald, *J. Am. Chem. Soc.* **1999**, *121*, 5805–5806; d) T. Cantat, L. Ricard, N. Mézailles, P. Le Floch, *Organometallics* **2006**, *25*, 6030–6038; e) R. P. Kamalesh Babu, R. McDonald, R. G. Cavell, *Chem. Commun.* **2000**, 481–482; f) N. D. Jones, G. Lin, R. A. Gossage, R. McDonald, R. G. Cavell, *Organometallics* **2003**, *22*, 2832–2841; g) G. Lin, N. D. Jones, R. A. Gossage, R. McDonald, R. G. Cavell, *Angew. Chem.* **2003**, *115*, 4188–4191; *Angew. Chem. Int. Ed.* **2003**, *42*, 4054–4057; h) T. Cantat, T. Arliguie, A. Noel, P. Thuéry, M. Ephritikhine, P. Le Floch, N. Mézailles, *J. Am. Chem. Soc.* **2009**, *131*, 963–972; i) J.-P. Tourneux, J.-C. Berthet, P. Thuéry, N. Mézailles, P. Le Floch, M. Ephritikhine, *Chem. Commun.* **2010**, *46*, 2494–2496; j) H. Heuclin, X. F. Le Goff, N. Mézailles, *Chem. Eur. J.* **2012**, *18*, 16136–16144; k) M. T. Gamer, M. Rastätter, P. W. Roesky, *Z. Anorg. Allg. Chem.* **2002**, *628*, 2269–2272; l) D P. Mills, O. J. Cooper, F. Tuna, E. J. L. McInnes, E. S. Davies, J. McMaster, F. Moro, W. Lewis, A. J. Blake, S. T. Liddle, *J. Am. Chem. Soc.* **2012**, *134*, 10047–10054; m) D. P. Mills, A. J. Wooles, J. McMaster, W. Lewis, A. J. Blake, S. T. Liddle, *Organometallics* **2009**, *28*, 6771–6776.

[5] M. Fustier, X. F. Le Goff, P. Le Floch, N. Mézailles, *J. Am. Chem. Soc.* **2010**, *132*, 13108–13110.

[6] a) D. P. Mills, L. Soutar, W. Lewis, A. J. Blake, S. T. Liddle, *J. Am. Chem. Soc.* **2010**, *132*, 14379–14381; b) D. P. Mills, W. Lewis, A. J. Blake, S. T. Liddle, *Organometallics* **2013**, *32*, 1239–1250; c) D. P. Mills, L. Soutar, O. J. Cooper, W. Lewis, A. J. Blake, S. T. Liddle, *Organometallics* **2013**, *32*, 1252–1264.

[7] T. E. Taylor, M. B. Hall, *J. Am. Chem. Soc.* **1984**, *106*, 1576–1584.

[8] a) A. Kasani, R. P. K. Babu, R. McDonald, R. G. Cavell, *Angew. Chem.* **1999**, *111*, 1580–1582; *Angew. Chem. Int. Ed.* **1999**, *38*, 1483–1484; b) L. Orzechowski, G. Jansen, S. Harder, *Angew. Chem.* **2009**, *121*, 3883–3887; *Angew. Chem. Int. Ed.* **2009**, *48*, 3825–3829; c) M. Demange, L. Boubekeur, A. Auffrant, N. Mézailles, L. Ricard, X. Le Goff, P. Le Floch, *New J. Chem.* **2006**, *30*, 1745–1754; d) L. Orzechowski, G. Jansen, S. Harder, *J. Am. Chem. Soc.* **2006**, *128*, 14676–14684; e) J. Vollhardt, H.-J. Gais, K. L. Lukas, *Angew. Chem.* **1985**, *97*, 607–609; *Angew. Chem. Int. Ed. Engl.* **1985**, *24*, 610–611; f) J. Vollhardt, H.-J. Gais, K. L. Lukas, *Angew. Chem.* **1985**, *97*, 695–697; *Angew. Chem. Int. Ed. Engl.* **1985**, *24*, 696–697; g) H.-J. Gais, J. Vollhardt, *J. Am. Chem. Soc.* **1988**, *110*, 978–980; h) J. F. K. Müller, M. Neuburger, M. Zehnder, *Helv. Chim. Acta* **1997**, *80*, 2182–2190; i) G. Linti, A. Rodig, H. Pritzkow, *Angew. Chem.* **2002**, *114*, 4685–4687; *Angew. Chem. Int. Ed.* **2002**, *41*, 4503–4506; j) J.-H. Chen, J. Guo, Y. Li, C.-W. So, *Organometallics* **2008**, *27*, 4617; k) O. J. Cooper, A. J. Wooles, J. McMaster, W. Lewis, A. J. Blake, S. T. Liddle, *Angew. Chem.* **2010**, *122*, 5702–5705; *Angew. Chem. Int. Ed.* **2010**, *49*, 5570–5573.

[9] P. Schröter, V. H. Gessner, *Chem. Eur. J.* **2012**, *18*, 11223–11227.

  

[10] V. H. Gessner, *Organometallics* **2011**, *30*, 4228–4231.
[11] H. Heuclin, M. Fustier-Boutignon, S. Ying-Fu Ho, X.-F. Le Goff, S. Carenco, C.-W. So, N. Mézailles, *Organometallics* **2013**, *32*, 498–508.
[12] Compound **1** has been synthesized before through an alternative reaction route: E. Payet, A. Auffrant, X. F. Le Goff, P. Le Floch, *J. Organomet. Chem.* **2010**, *695*, 1499–1506.
[13] T. Cantat, L. Ricard, P. Le Floch, N. Mézailles, *Organometallics* **2006**, *25*, 4965–4976.
[14] a) T. Stey, D. Stalke in *The Chemistry of Organolithium Compounds* (Eds.: Z. Rappoport, I. Marek),Wiley, Chichester, **2004**, p. 47–120; b) V. H. Gessner, C. Däschlein, C. Stohmann, *Chem. Eur. J.* **2009**, *15*, 3320–3335.
[15] T. Cantat, N. Mézailles, Y. Jean, P. Le Floch, *Angew. Chem.* **2004**, *116*, 6542–6545; *Angew. Chem. Int. Ed.* **2004**, *43*, 6382–6385.
[16] H. V. Huynh, Y. Han, R. Jothibasu, J. A. Yang, *Organometallics* **2009**, *28*, 5395–5404.
[17] *Multinuclear NMR* (Ed.: J. Mason), Plenum Press, New York, **1987**.
[18] S. F. Vyboishchikov, G. Frenking, *Chem. Eur. J.* **1998**, *4*, 1428–1438.
[19] For examples of further calculations on Schrock- and Fischer carbene complexes, see: a) G. Occhipinti, V. R. Jensen, *Organometallics* **2011**, *30*, 3522–3529; b) G. Occhipinti, H.-R. Bjørsvik, V. R. Jensen, *J. Am. Chem. Soc.* **2006**, *128*, 6952.
[20] a) G. Frenking, M. Solà, S. F. Vyboishchikov, *J. Organomet. Chem.* **2005**, *690*, 6178–6204; b) M. Cases, G. Frenking, M. Duran, M. Solà, *Organometallics* **2002**, *21*, 4182–4191; c) D. Nemcsok, K. Wichmann, G. Frenking, *Organometallics* **2004**, *23*, 3640–3646.
[21] The palladium–carbene complex differs from all other complexes in that way that the HOMO displays an antibonding π-type interaction. Because of the filled d orbitals, no free orbital is available to allow for a bonding interaction.
[22] C. Elschenbroich, *Organometallchemie*, 4th ed., Teubner, Stuttgart, **2003**, p. 313.
[23] O. J. Cooper, D. P. Mills, J. McMaster, F. Tuna, E. J. L. McInnes, W. Lewis, A. J. Blake, S. T. Liddle, *Chem. Eur. J.* **2013**, *19*, 7071–7083.
[24] R. F. W. Bader, *Atoms in Molecules: A Quantum Theory*, Oxford University Press, Oxford, **1990**.
[25] Y. Smurnyy, C. Bibal, M. Pink, K. G. Caulton, *Organometallics* **2005**, *24*, 3849–3855.
[26] L. Mayer, *Chem. Ber.* **1961**, *94*, 3056.
[27] a) SAINT v7.68A in Bruker APEX v2011.9, Bruker AXS Inst. Inc., Madison, WI, USA, **2008**; b) G. M. Sheldrick, SADABS 2008/2; Universität Göttingen, Göttingen, Germany, **2008**; c) G. M. Sheldrick, *Acta Cryst., Sect. A* **1990**, *46*, 467–473; d) G. M. Sheldrick, *Acta Cryst., Sect. A* **2008**, *64*, 112–122.
[28] a) Gaussian 03, Revision E.01, M. J. Frisch, G. W. Trucks, H. B. Schlegel, G. E. Scuseria, M. A. Robb, J. R. Cheeseman, J. A. Montgomery, Jr., T. Vreven, K. N. Kudin, J. C. Burant, J. M. Millam, S. S. Iyengar, J. Tomasi, V. Barone, B. Mennucci, M. Cossi, G. Scalmani, N. Rega, G. A. Petersson, H. Nakatsuji, M. Hada, M. Ehara, K. Toyota, R. Fukuda, J. Hasegawa, M. Ishida, T. Nakajima, Y. Honda, O. Kitao, H. Nakai, M. Klene, X. Li, J. E. Knox, H. P. Hratchian, J. B. Cross, V. Bakken, C. Adamo, J. Jaramillo, R. Gomperts, R. E. Stratmann, O. Yazyev, A. J. Austin, R. Cammi, C. Pomelli, J. W. Ochterski, P. Y. Ayala, K. Morokuma, G. A. Voth, P. Salvador, J. J. Dannenberg, V. G. Zakrzewski, S. Dapprich, A. D. Daniels, M. C. Strain, O. Farkas, D. K. Malick, A. D. Rabuck, K. Raghavachari, J. B. Foresman, J. V. Ortiz, Q. Cui, A. G. Baboul, S. Clifford, J. Cioslowski, B. B. Stefanov, G. Liu, A. Liashenko, P. Piskorz, I. Komaromi, R. L. Martin, D. J. Fox, T. Keith, M. A. Al-Laham, C. Y. Peng, A. Nanayakkara, M. Challacombe, P. M. W. Gill, B. Johnson, W. Chen, M. W. Wong, C. Gonzalez, J. A. Pople, Gaussian, Inc., Wallingford CT, **2004**; b) NBO 5.G, E. D. Glendening, J. K. Badenhoop, A. E. Reed, J. E. Carpenter, J. A. Bohmann, C. M. Morales, F. Weinhold, Theoretical Chemistry Institute, University of Wisconsin, Madison, **2001**, http://www.chem.wisc.edu/~nbo5.
[29] a) A. D. Becke, *Phys. Rev. A* **1988**, *38*, 3098–3100; b) P. Perdew, *Phys. Rev. B* **1986**, *33*, 8822–8824.
[30] L. E. Roy, P. J. Hay, R. L. Martin, *J. Chem. Theory Comput.* **2008**, *4*, 1029–1031.
[31] A. W. Ehlers, M. Böhme, S. Dapprich, A. Gobbi, A. Höllwarth, V. Jonas, K. F. Köhler, R. Stegman, A. Veldkamp, G. Frenking, *Chem. Phys. Lett.* **1993**, *208*, 111–114.
[32] M. Kohout, DGrid, version 4.6, Radebeul, **2011**.
[33] a) A. D. Becke, K. E. Edgecombe, *J. Chem. Phys.* **1990**, *92*, 5397–5403; b) A. Savin, O. Jepsen, J. Flad, O. K. Andersen, H. Preuss, H. G. Vonschnering, *Angew. Chem.* **1992**, *104*, 186–188; *Angew. Chem. Int. Ed. Engl.* **1992**, *31*, 187–188; c) M. Kohout, A. Savin, *Int. J. Quantum Chem.* **1996**, *60*, 875–882.
[34] Paraview, version 3.8, Kitware Inc., Clifton Park, New York, **2010**; available from http://www.paraview.org.
[35] Amsterdam Density Functional (ADF), version 2012.01, SCM, Theoretical Chemistry, Vrije Univeriteit, Amsterdam, Netherlands, **2012**; available from http://www.scm.com.
[36] a) A. D. Becke, *J. Chem. Phys.* **1993**, *98*, 5648–5652; b) C. T. Lee, W. T. Yang, R. G. Parr, *Phys. Rev. B* **1988**, *37*, 785–789.
[37] a) S. K. Wolff, T. Ziegler, *J. Chem. Phys.* **1998**, *109*, 895–905; b) S. K. Wolff, T. Ziegler, E. van Lenthe, E. J. Baerends, *J. Chem. Phys.* **1999**, *110*, 7689–7698. For a recent survey of relativistic DFT calculations of NMR parameters, see also: J. Autschbach, S. Zheng, *Annu. Rep. NMR Spectrosc.* **2009**, *67*, 1–95.
[38] K. Wolinski, J. F. Hinton, P. Pulay, *J. Am. Chem. Soc.* **1990**, *112*, 8251–8260.
[39] Gaussian 09, Revision A.02, M. J. Frisch, G. W. Trucks, H. B. Schlegel, G. E. Scuseria, M. A. Robb, J. R. Cheeseman, G. Scalmani, V. Barone, B. Mennucci, G. A. Petersson, H. Nakatsuji, M. Caricato, X. Li, H. P. Hratchian, A. F. Izmaylov, J. Bloino, G. Zheng, J. L. Sonnenberg, M. Hada, M. Ehara, K. Toyota, R. Fukuda, J. Hasegawa, M. Ishida, T. Nakajima, Y. Honda, O. Kitao, H. Nakai, T. Vreven, J. A. Montgomery, Jr., J. E. Peralta, F. Ogliaro, M. Bearpark, J. J. Heyd, E. Brothers, K. N. Kudin, V. N. Staroverov, R. Kobayashi, J. Normand, K. Raghavachari, A. Rendell, J. C. Burant, S. S. Iyengar, J. Tomasi, M. Cossi, N. Rega, J. M. Millam, M. Klene, J. E. Knox, J. B. Cross, V. Bakken, C. Adamo, J. Jaramillo, R. Gomperts, R. E. Stratmann, O. Yazyev, A. J. Austin, R. Cammi, C. Pomelli, J. W. Ochterski, R. L. Martin, K. Morokuma, V. G. Zakrzewski, G. A. Voth, P. Salvador, J. J. Dannenberg, S. Dapprich, A. D. Daniels, Ö. Farkas, J. B. Foresman, J. V. Ortiz, J. Cioslowski, D. J. Fox, Gaussian, Inc., Wallingford CT, **2009**.
[40] a) D. Andrae, U. Haeussermann, M. Dolg, H. Stoll, H. Preuss, *Theor. Chim. Acta* **1990**, *77*, 123; b) J.M.L. Martin, A. Sundermann, *J. Chem. Phys.* **2001**, *114*, 3408.
[41] W. Kutzelnigg, U. Fleischer, M. Schindler, in *NMR Basic Principles and Progress, Vol. 23: Deuterium and Shift Calculation* (Eds.: P. Diehl, E. Fluck, H. Günther, R. Kosfeld, J. Seelig), *The IGLO-Method: Ab Initio Calculation and Interpretation of NMR Chemical Shifts and Magnetic Susceptibilities*, Springer, Berlin, **1991**, pp. 165–262.
[42] V. G. Malkin, O. L. Malkina, R. Reviakine, A. V. Arbuznikov, M. Kaupp, B. Schimmelpfennig, I. Malkin, M. Repisky, S. Komorovsky, P. Hrobarik, E. Malkin, T. Helgaker, K. Ruud, *MAG-ReSpect*, version 2.1, **2005**.
[43] J. Pipek, P. G. Mezey, *J. Chem. Phys.* **1989**, *90*, 4916.
[44] U. Varetto, *Molekel, version 5.4*, Swiss National Supercomputing Center, Manno, Switzerland; available from: http://molekel.cscs.ch.

Received: August 6, 2013
Published online: October 21, 2013

  